

Supporting information

Polymerizable deep eutectic solvents-based mechanically strong and ultra-stretchable conductive elastomers for detecting human motions

Kaili Zhang,^{‡a} Ren'ai Li,^{‡a} Guangxue Chen,^{‡a} Jimin Yang,^b Junfei Tian,^a Minghui He^{*a}

^a State Key Laboratory of Pulp and Paper Engineering, School of Light Industry and Engineering, South China University of Technology, Guangzhou 510640, China.

^b Guangzhou Banknote Printing CO. Ltd., Guangzhou 510530, China.

[‡] These authors contributed equally to this work.

* Corresponding author's E-mail: heminghui@scut.edu.cn

Experimental Section

Materials

Tetramethylammonium chloride (TMAC, >99%, Shanghai Aladdin Bio-Chem Technology Co., Ltd.), acrylic acid (AA, >99%, Shanghai Macklin Biochemical Co., Ltd.), phytic acid solution (PA, 50 wt.% in H₂O, Shanghai Aladdin Bio-Chem Technology Co., Ltd.), poly(ethylene glycol)diacrylate (PEG(200)DA, Shanghai Aladdin Bio-Chem Technology Co., Ltd.), and 2-hydroxy-4-(2-hydroxyethoxy)-2-methylpropiophenone (photo-initiator 2959, ≥98%, Tianjin Jiuri New Materials) were used as received.

Fabrication of TMAC-AA type PDES

TMAC as the ammonium salt should be dried under vacuum at 65°C for 2 hours. TMAC and AA were mixed in 1:2 mole ratio. Then, the mixture was heated and stirred at 75°C in a closed flask until a homogenous colorless solution was formed. The prepared PDES was then kept in a vacuum desiccator with silica gel until further use.

Photopolymerization of TMAC-AA-PA type PDES

Various amount of PA was added into TMAC-AA PDES and stirred vigorously until a transparent solution was formed at room temperature. Then, 0.1 mol% crosslinkers PEG(200)DA and 0.1 mol% photo-initiator 2959 to AA monomer were added into the resulting TMAC-AA type PDESs. The mixed solution was stirring at room temperature until a homogenous colorless solution was formed. Finally, the precure solutions were fabricated and kept in a vacuum desiccator with silica gel until further use.

For preparing CE, the precursor solution was injected into two release films coated glasses mold sandwiched with a silicon film, and thickness and shape were determined by silicon film. Then the reaction was initiated by a UV light source (RW-UVA-Φ200U, Shenzhen Runwing Company, China) with a dominant wavelength of 365 nm for 2 min. The light intensity was 20 mW·cm⁻² measured by the UV radiometer.

Preparation of a strain sensor

The CE was cut into the size of $2 \times 1 \times \text{thickness cm}^3$ and copper wires were attached on two ends of the CE by tapes for electrical signal transmission. It is important to note that we used 1 mm CEs to detect the human motion owing to its strong mechanical properties and load-bearing capacity, while the 0.1 mm CE were used to detect the motion of human joints because of their favorable flexibility. When performing tests, the strain sensor was in series with a Keithley DMM7510 source meter to detect the motion of the volunteer.

Measuring the conductivity of the CEs

The measuring system and the instrument was PGSTAT 302N (Princeton Applied Research). Current ranging was 200 mA, and the frequency range was from 1 Hz to 10^5 Hz. The samples were cut into 1 cm (width) \times 1 cm (length) \times thickness, and sandwiched by copper tapes. The testing condition was at room temperature 25 °C and the humidity was about 35%. The values of conductivity were calculated from the impedance curves.

The CEs in our paper were resistive type strain sensors. And the resistance was determined by the formula (1),

$$R = \rho * L/S \quad (1)$$

where R represented the resistance, ρ represented the resistivity, L represented the length of the CE and S represented area. During the deformation, the L and S of the CE increase or decrease accordingly, resulting in a change in resistance. As a result, the DMM7510 records the real-time resistance value.

Characterizations

Fourier transform infrared (FTIR) spectra were recorded on a Bruker Vertex 33 spectrometer. ^1H NMR spectra (400 MHz) were tested using a Bruker spectrometer AVANCE III HD 400. Chloroform (CDCl_3) was used as external reference. The surface morphologies of polymeric films were observed using AFM (Bruker Multimode 8) with the tapping mode. Differential scanning calorimeter (DSC) was employed at a heating rate of 10 °C/min under nitrogen atmosphere (DSC 214 Polymer). The regular light transmittance was tested by the UV-visible spectrometer (Cary60, Agilent, USA). The wavelength range was 200-800 nm with a speed of 600 nm/min. The tensile testing was performed by using a tensile machine (INSTRON 5565). The tensile speed was set to 10 mm/min. The electrochemical properties were measured by PGSTAT 302N (Princeton Applied Research) through

an AC impedance method. The applied frequency range in the electrical tests was from 1 to 10^5 Hz. The optical microscope images of the cutting CE after self-healing were recorded on a polarized optical microscope (OLYMPUS, BX63). The current signals of sensors were measured in real-time with a Keithley DMM7510 source meter. Optical images were taken by a Nikon Digital Sight DS-Fil camera. The testing conditions was at room temperature 25°C and the humidity was about 35%.

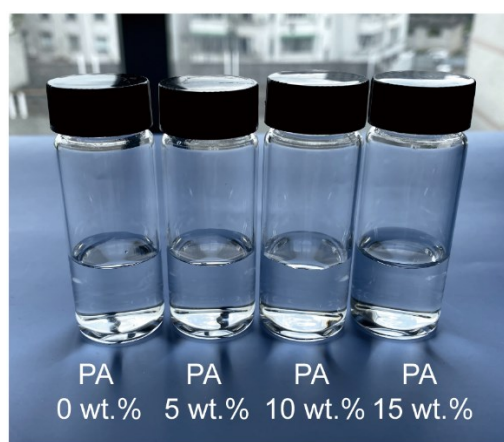


Figure S1. Optical photograph of TMAC-AA-PA type PDESs with different amount of PA.

Table S1. The detailed components of diverse PDESs.

PDES preparation	PA (wt.%) to PDES	Photopolymerization for 2 min
TMAC:AA=1:2 (mole ratio)	0	Transparent elastomer, rigid
	5	Transparent elastomer, tough
	10	Transparent elastomer, tough
	15	Transparent elastomer, soft

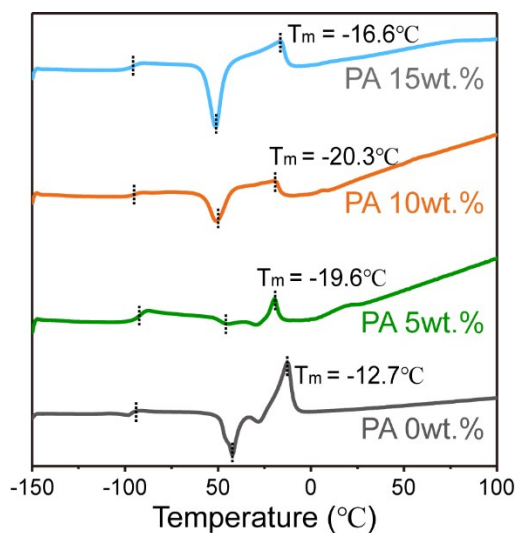


Figure S2. DSC traces of TMAC-AA-PA type PDESs with different amount of PA.

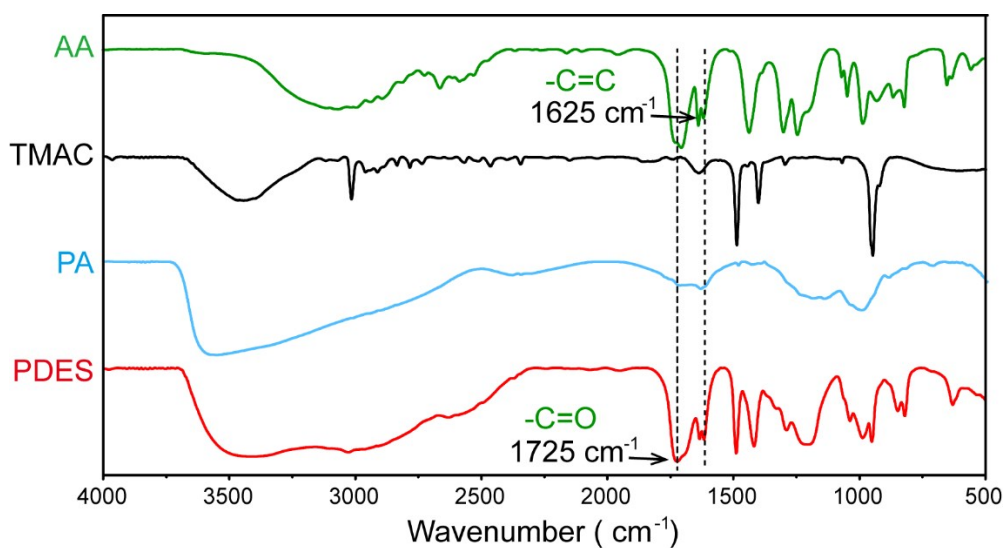


Figure S3. The FTIR spectroscopy of AA, TMAC, PA and TMAC-AA-PA type PDES, respectively.

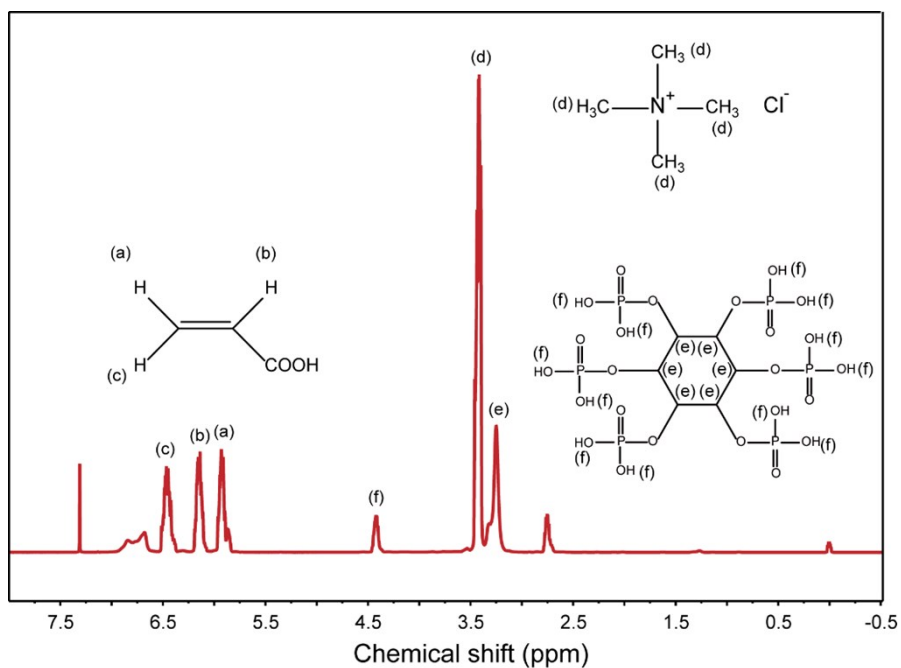


Figure S4. ^1H NMR spectrum of TMAC-AA-PA type PDES.

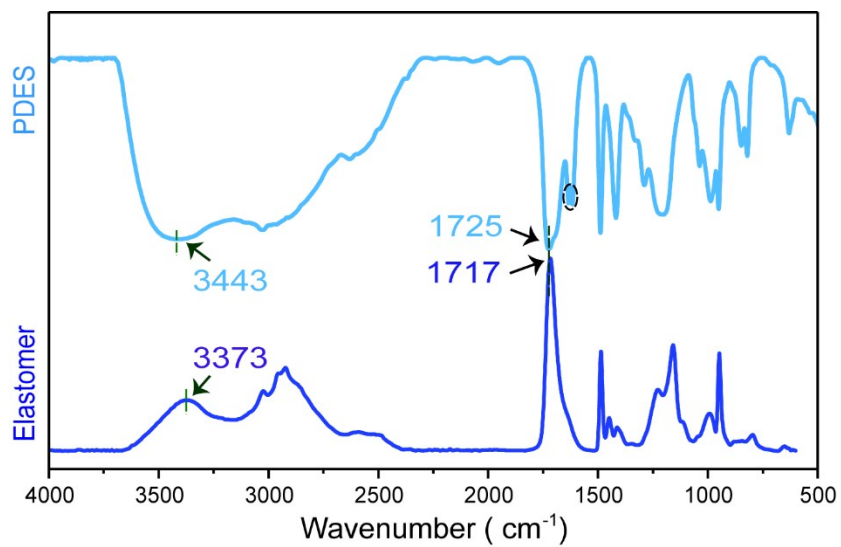


Figure S5. The FTIR spectroscopy of TMAC-AA-PA type PDES before (up) and after (down) photopolymerization.

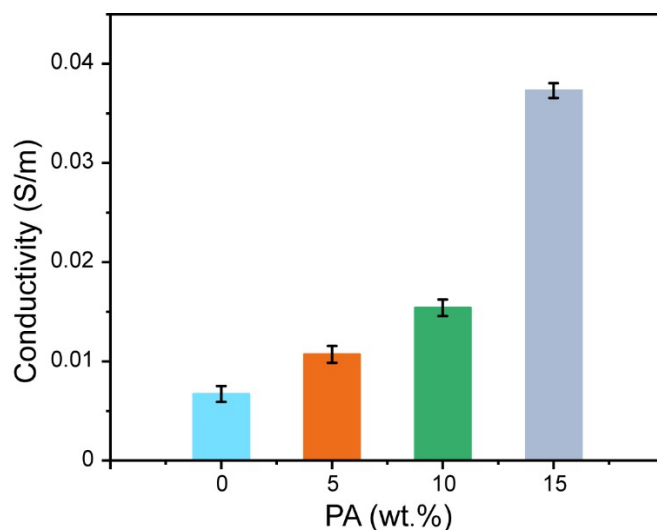


Figure S6. The conductivity of CESs with different PA content.

Table S2. The conductivity of the PDESs and corresponding elastomers.

Conductivity (S/m)	The amount of PA	0 wt.%	5 wt.%	10 wt.%	15 wt.%
	PDES		~0.395	~0.473	~0.495
Elastomer		~0.007	~0.011	~0.015	~0.037

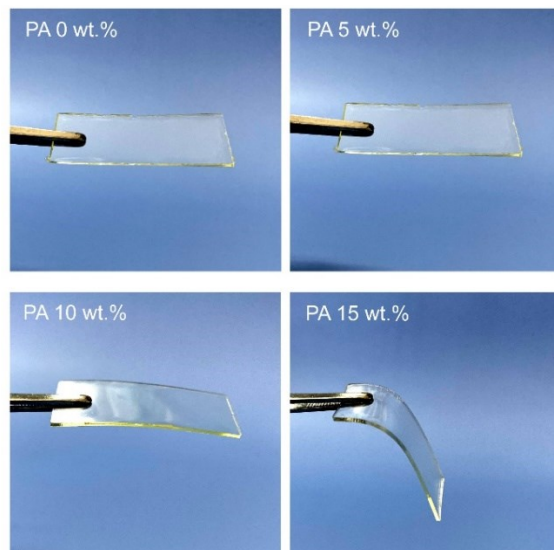


Figure S7. Digital images of CEs with different PA contents.



Figure S8. Digital image of a fragile CE without PA.

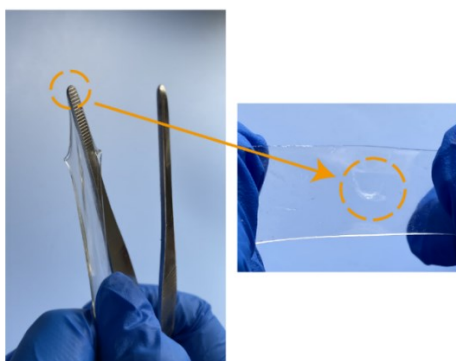


Figure S9. Digital image for CE with 10 wt.% PA that can tolerate puncture.



9500 X

Figure S10. Photos of lifting a 10.5 kg weight (9500 times its own weight) by a CE with 10 wt.% PA.

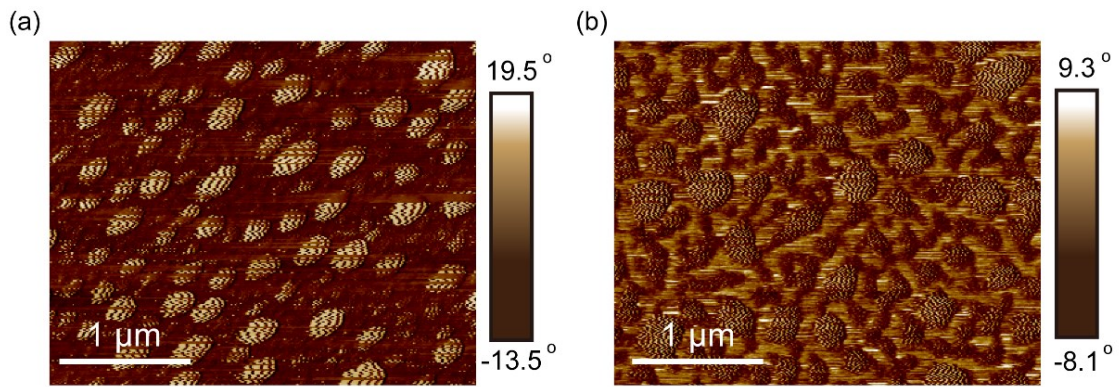


Figure S11. AFM phase images of CE with (a) 0 wt.% and (b) 10 wt.% PA content.

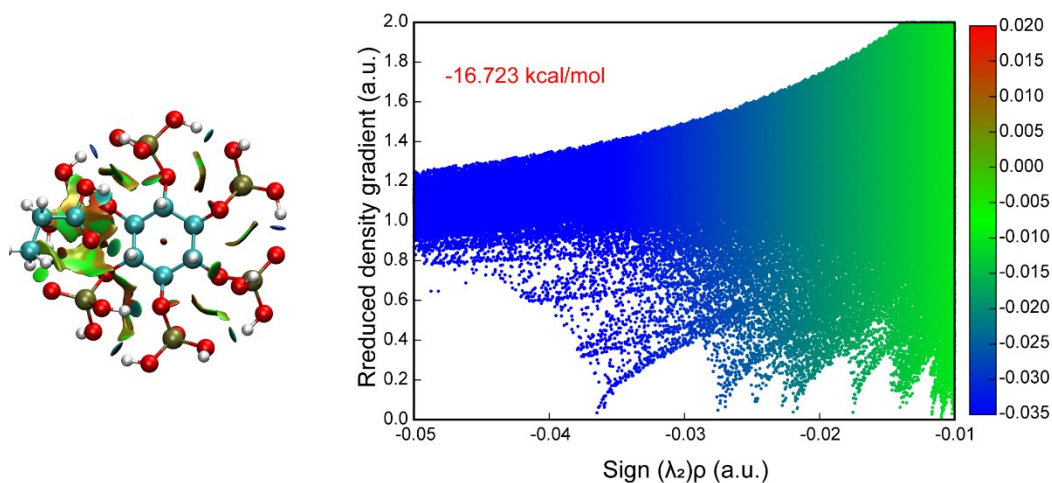


Figure S12. RDG vs $\text{sign}(\lambda_2)\rho$ for PA and AA.

Table S3. Tensile strength strain-at-break, and toughness for CEs with different amount of PA.

The amount of PA	Tensile strength	Strain-at-break	Toughness
0	82.05 MPa	22%	12 MJ*m ⁻³
5 wt.%	66.41 MPa	42%	19 MJ*m ⁻³
10 wt.%	31.21 MPa	3645%	615 MJ*m ⁻³
15 wt.%	4.39 MPa	6164%	149 MJ*m ⁻³

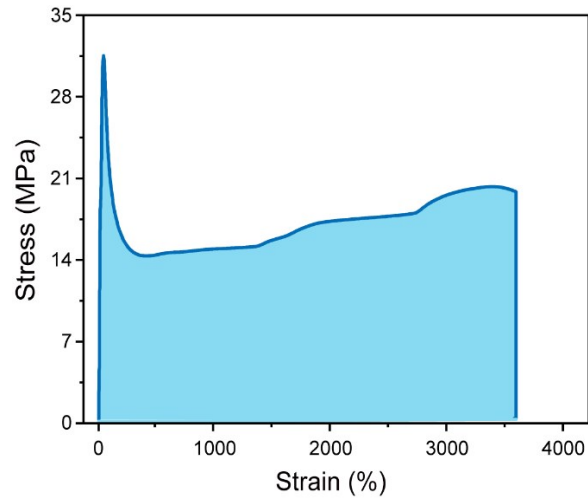


Figure S13. The toughness of the CE with 10 wt.% PA.

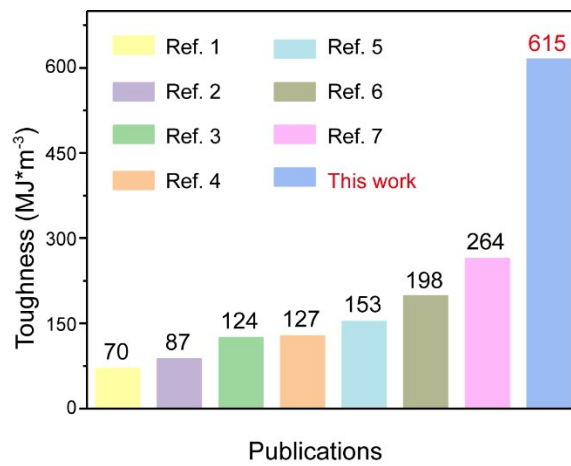


Figure S14. The toughness of the mechanically strong elastomers in recent works.¹⁻⁷

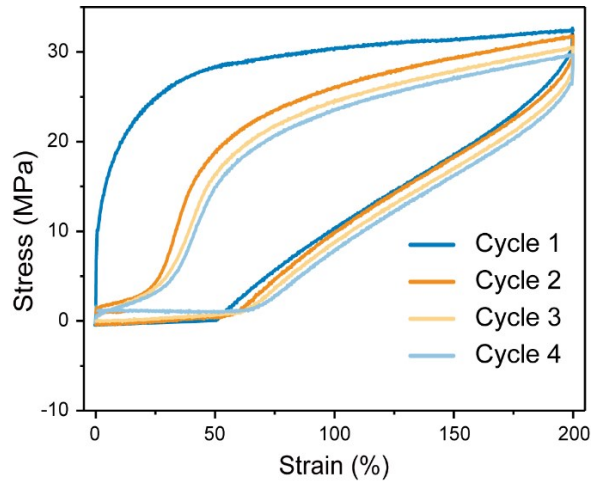


Figure S15. Cyclic stress-strain curves of the CE with 10 wt.% PA.

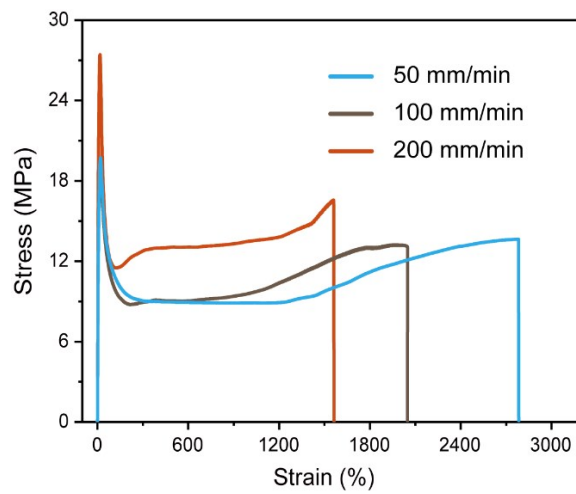


Figure S16. Tensile stress-strain curves of the CE with 10 wt.% PA under different tensile speed.

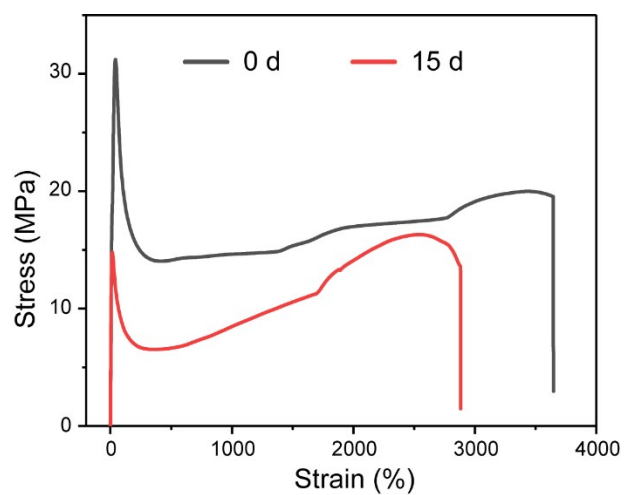


Figure S17. Mechanical stability of the CE with 10 wt.% PA as the evolution of time.

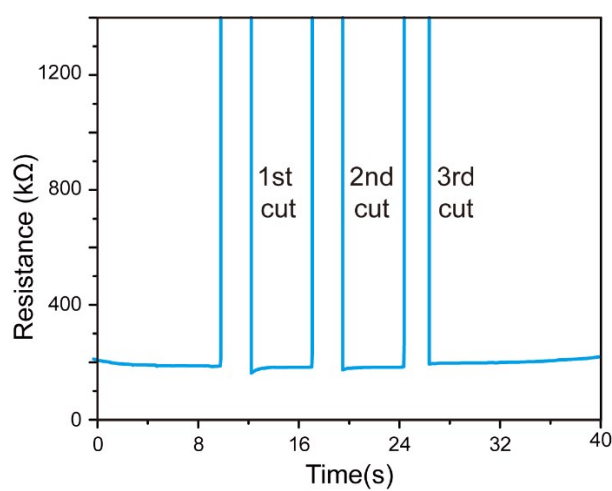


Figure S18. The resistance of the CE with 10 wt.% PA before cut and after self-healing.

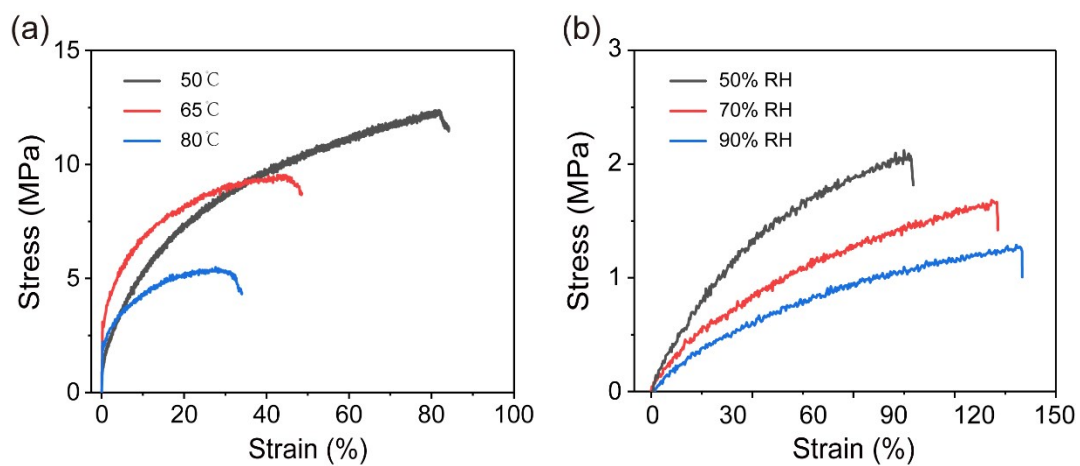


Figure S19. The stress-strain curve of the healed CE with 10 wt.% PA under different temperature and humidity.

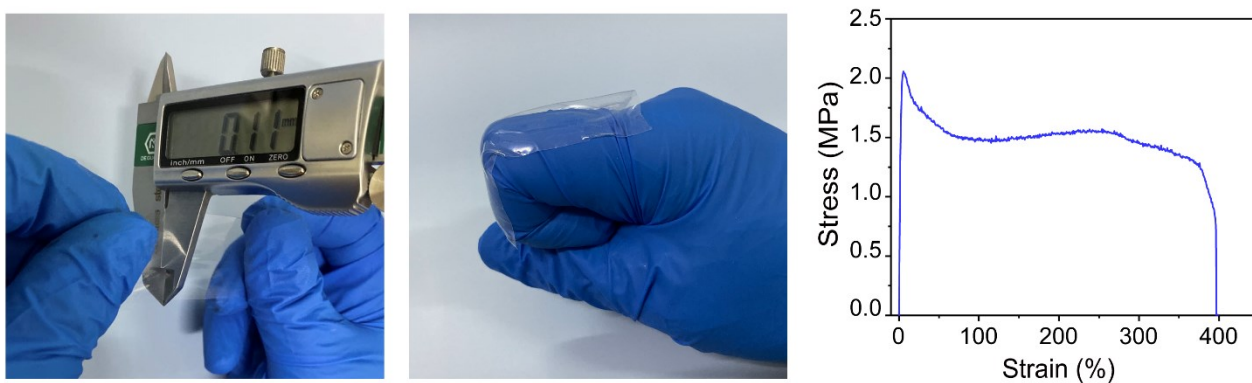


Figure S20. Extremely thin elastomer (0.11 mm) and its corresponding stress-strain curve.

References:

1. Y. Miwa, J. Kurachi, Y. Kohbara and S. Kutsumizu, *Communications Chemistry*, 2018, **1**, 5.
2. L. Zhang, *Advanced Materials*, 2019, **31**, 1901402.
3. B. Qin, S. Zhang, P. Sun, B. Tang, Z. Yin, X. Cao, Q. Chen, J.F. Xu and X. Zhang, *Advanced Materials*, 2020, **10**, 2000096.
4. Z. Shi, J. Kang and L. Zhang, *ACS Applied Materials & Interfaces*, 2020, **12**, 23484-23493.
5. D. Wan, Q. Jiang, Y. Song, J. Pan, T. Qi and G. L. Li, *ACS Applied Polymer Materials*, 2020, **2**, 879-886.
6. N. Duan, Z. Sun, Y. Ren, Z. Liu, L. Liu and F. Yan, *Polymer Chemistry*, 2020, **11**, 867-875.
7. W. Liu, C. Fang, S. Wang, J. Huang and X. Qiu, *Macromolecules*, 2019, **52**, 6474-6484.